Fine Structure Constant Defines Visual Transparency of Graphene

R. R. Nair,[1] P. Blake,[1] A. N. Grigorenko,[1] K. S. Novoselov,[1] T. J. Booth,[1] T. Stauber,[2] N. M. R. Peres,[2] A. K. Geim[1]*

There are few phenomena in condensed matter physics that are defined only by the fundamental constants and do not depend on material parameters. Examples are the resistivity quantum, h/e^2, that appears in a variety of transport experiments, including the quantum Hall effect and universal conductance fluctuations, and the magnetic flux quantum, $h/2e$, playing an important role in the physics of superconductivity (h is Planck's constant and e the electron charge). By and large, it requires sophisticated facilities and special measurement conditions to observe any of these phenomena. In contrast, we show that the opacity of suspended graphene (*1*) is defined solely by the fine structure constant, $\alpha = e^2/\hbar c \approx 1/137$ (where c is the speed of light), the parameter that describes coupling between light and relativistic electrons and that is traditionally associated with quantum electrodynamics rather than materials science. Despite being only one atom thick, graphene is found to absorb a significant ($\pi\alpha = 2.3\%$) fraction of incident white light, a consequence of graphene's unique electronic structure.

It was recently argued (*2*, *3*) that the high-frequency (dynamic) conductivity G for Dirac fermions (*1*) in graphene should be a universal constant equal to $e^2/4\hbar$ and different from its universal dc conductivity, $4e^2/\pi h$ [however, the experiments do not comply with the prediction for dc conductivity (*1*)]. The universal G implies (*4*) that observable quantities such as graphene's optical transmittance T and reflectance R are also universal and given by $T \equiv (1 + 2\pi G/c)^{-2} = (1 + \frac{1}{2}\pi\alpha)^{-2}$ and $R \equiv \frac{1}{4}\pi^2\alpha^2 T$ for the normal light incidence. In particular, this yields graphene's opacity $(1 - T) \approx \pi\alpha$ [this expression can also be derived by calculating the absorption of light by two-dimensional Dirac fermions with Fermi's golden rule (*5*)]. The origin of the optical properties being defined by the fundamental constants lies in the two-dimensional nature and gapless electronic spectrum of graphene and does not directly involve the chirality of its charge carriers (*5*).

We have studied specially prepared graphene crystals (*5*) such that they covered submillimeter apertures in a metal scaffold (Fig. 1A inset). Such large one-atom-thick membranes suitable for optical studies were previously inaccessible (*6*). Figure 1A shows an image of one of our samples in transmitted white light. In this case, we have chosen to show an aperture that is only partially covered by suspended graphene so that opacities of different areas can be compared. The line scan across the image qualitatively illustrates changes in the observed light intensity. Further measurements (*5*) yield graphene's opacity of $2.3 \pm 0.1\%$ and negligible reflectance (<0.1%), whereas optical spectroscopy shows that the opacity is practically independent of wavelength, λ (Fig. 1B) (*5*). The opacity is found to increase with membranes' thickness so that each graphene layer adds another 2.3% (Fig. 1B inset). Our measurements also yield a universal dynamic conductivity $G = (1.01 \pm 0.04)\ e^2/4\hbar$ over the visible frequencies range (*5*), that is, the behavior expected for ideal Dirac fermions.

The agreement between the experiment and theory is striking because it was believed that the universality could hold only for low energies ($E < 1$ eV), beyond which the electronic spectrum of graphene becomes strongly warped and nonlinear and the approximation of Dirac fermions breaks down. However, our calculations (*5*) show that finite-E corrections are surprisingly small (a few %) even for visible light. Because of these corrections, a metrological accuracy for α would be difficult to achieve, but it is remarkable that the fine structure constant can so directly be assessed practically by the naked eye.

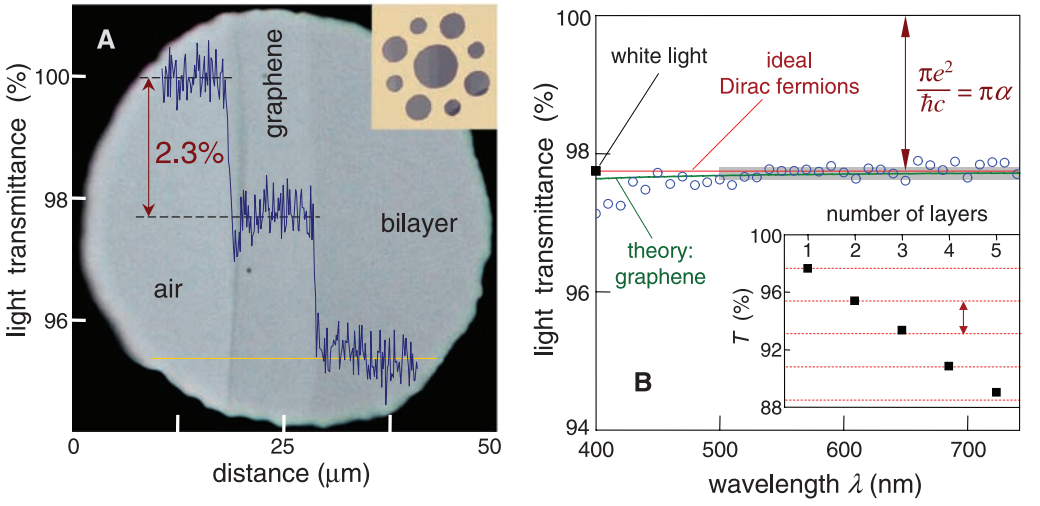

Fig. 1. Looking through one-atom-thick crystals. (**A**) Photograph of a 50-μm aperture partially covered by graphene and its bilayer. The line scan profile shows the intensity of transmitted white light along the yellow line. (Inset) Our sample design: A 20-μm-thick metal support structure has several apertures of 20, 30, and 50 μm in diameter with graphene crystallites placed over them. (**B**) Transmittance spectrum of single-layer graphene (open circles). Slightly lower transmittance for $\lambda < 500$ nm is probably due to hydrocarbon contamination (*5*). The red line is the transmittance $T = (1 + 0.5\pi\alpha)^{-2}$ expected for two-dimensional Dirac fermions, whereas the green curve takes into account a nonlinearity and triangular warping of graphene's electronic spectrum. The gray area indicates the standard error for our measurements (*5*). (Inset) Transmittance of white light as a function of the number of graphene layers (squares). The dashed lines correspond to an intensity reduction by $\pi\alpha$ with each added layer.

References and Notes

1. A. K. Geim, K. S. Novoselov, *Nat. Mater.* **6**, 183 (2007).
2. T. Ando, Y. Zheng, H. Suzuura, *J. Phys. Soc. Jpn.* **71**, 1318 (2002).
3. V. P. Gusynin, S. G. Sharapov, J. P. Carbotte, *Phys. Rev. Lett.* **96**, 256802 (2006).
4. A. B. Kuzmenko, E. van Heumen, F. Carbone, D. van der Marel, *Phys. Rev. Lett.* **100**, 117401 (2008).
5. Materials and methods are available on *Science* Online.
6. J. S. Bunch *et al.*, *Science* **315**, 490 (2007).

7. We are grateful to A. Kuzmenko, A. Castro Neto, P. Kim, and L. Eaves for illuminating discussions. Supported by Engineering and Physical Sciences Research Council (UK), the Royal Society, European Science Foundation, and Office of Naval Research.

Supporting Online Material

www.sciencemag.org/cgi/content/full/1156965/DC1
Materials and Methods
SOM Text
Figs. S1 to S5
References

25 February 2008; accepted 26 March 2008
Published online 3 April 2008;
10.1126/science.1156965
Include this information when citing this paper.

[1]Manchester Centre for Mesoscience and Nanotechnology, University of Manchester, M13 9PL Manchester, UK. [2]Department of Physics, University of Minho, P-4710-057 Braga, Portugal.

*To whom correspondence should be addressed. E-mail: geim@man.ac.uk

www.sciencemag.org/cgi/content/full/1156965/DC1

Supporting Online Material for

Fine Structure Constant Defines Visual Transparency of Graphene

R. R. Nair, P. Blake, A. N. Grigorenko, K. S. Novoselov, T. J. Booth, T. Stauber, N. M. R. Peres, A. K. Geim*
*To whom correspondence should be addressed. E-mail: geim@man.ac.uk

Published 3 April 2008 on *Science* Express
DOI: 10.1126/science.1156965

This PDF file includes:

Supplementary Online Material for manuscript

"Fine Structure Constant Defines Visual Transparency of Graphene"

by Nair *et al*

MATERIALS AND METHODS

Fabrication of graphene membranes

Large graphene crystals were prepared by micromechanical cleavage of natural graphite (www.graphit.de) on top of an oxidized Si wafer (*S1*) with an additional thin layer of PMMA (*S2*). The latter significantly improved adhesion and allowed us to make graphene monocrystals that could easily exceed 100 μm in size. We used NITTO tape to minimize contamination by adhesive residues. Single-, double- or few-layer crystallites were identified in an optical microscope due to their different contrast that increases with increasing the number of layers (*S2*). The number of layers was also verified with atomic force and Raman microscopy.

By using photolithography, a perforated 20-μm-thick copper-gold film was deposited on top of the found crystallites. The films usually had 9 small apertures with diameters 20, 30 and 50 μm (see inset of Fig. 1A and Fig. S1), and the graphene crystallites were aligned against the apertures to cover them completely or partially. The Cu/Au film also served as a support structure (scaffold) and was 3 mm in diameter so that it could be used in standard holders for transmission electron microscopy (TEM). At the final stage of microfabrication, the scaffold was lifted off by dissolving the sacrificial PMMA layer, which left graphene attached to the scaffold (the use of a critical point dryer was essential).

The resulting devices could easily be handled and transferred between different measurement facilities. The developed technique allows a reliable and routine fabrication of practically macroscopic graphene membranes suitable for optical, electron-microscopy or other studies (our success rate in making the final devices is >50%). This is a significant technological advance with respect to the earlier fabrication procedures that largely relied on chance and allowed graphene membranes of only a few microns in size (*S3*,*S4*).

Optical measurements

To measure the optical spectra, we used a xenon lamp (250-1200nm) as a light source and focused its beam on graphene membranes. The transmitted light intensity was measured by Ocean Optics HR2000 spectrometer. The recorded signal was then compared with the one obtained by directing the light beam through either an empty space or, as a double check, another aperture of the same size but without graphene. Typical experimental data are shown in Figure S2 by open circles. Here, to reduce the measurement noise below 0.1%, we have averaged the spectral curves over intervals $\Delta\lambda$ of 10 nm.

An interesting alternative method to measure optical spectra of graphene was to use membranes that only partially covered the apertures (such as shown in Fig. S1) and take their images in an optical microscope (we used Nikon Eclipse LV100) using 22 different narrow-band-pass filters for transmission illumination. The images taken by high-quality grey and color cameras (Nikon DS2MBW and DS2Mv) were then analyzed, and

relative intensities of the light transmitted through different areas were calculated. Examples of such spectroscopy for graphene and its bilayer are shown in Fig. S3. Results of the two measurement techniques are compared in Figure S2 (circles versus squares) and show nearly the same accuracy. Note that the use of an optical microscope is possible for graphene membranes because they mostly absorb light with only a minute portion of it being reflected (<0.1%). The latter ensures that the opacity of graphene is practically independent of the numerical aperture and magnification (this was carefully checked experimentally and is in agreement with our calculations).

Both approaches to measure graphene transmittance spectra show a deviation from a constant opacity for $\lambda <$ 500 nm (photon energy $E >$2.5eV), and the same is valid for bilayer graphene (see Fig. 1B, S2 and S3). Such rapid deviations are not expected in theory (see below). We have investigated this spectral feature further and found that it is connected with surface contamination of graphene membranes by hydrocarbons. Graphene is extremely lipophilic and hydrocarbon contamination is practically impossible to avoid for samples exposed to air (a hydrocarbon layer partially covering graphene is always found in TEM; see, for example, ref. (*S3*)). To this end, we annealed our membranes in a hydrogen-argon atmosphere (*S5*) at 200C°, which significantly improved their cleanliness, as observed in TEM by using the membranes immediately after their annealing. The annealing is also found to significantly weaken the downturn in the violet-light transmittance but did not affect the spectra for $\lambda >$500nm, which indicates that hydrocarbons are indeed responsible for this additional opacity (or, at least, most of it). Here we note that many polymer (hydrocarbon) materials, especially those used in lithography, have an absorption edge in violet light. Alternatively, we speculate that it could be a tail of the plasmon resonance expected at $E \approx$5eV, which is broadened by surface contaminants.

SUPPLEMENTARY TEXT

Universal dynamic conductivity of graphene

Optical properties of thin films are commonly described in terms of dynamic or optical conductivity G. For a two-dimensional (2D) Dirac spectrum with a conical dispersion relation $\varepsilon = \hbar v_F |\boldsymbol{k}|$ ($v_F \approx 10^6$m/s is the Fermi velocity and $\boldsymbol{k}$ the wavevector), G was theoretically predicted (*S6- S10*) to exhibit a universal value $G_0 \equiv e^2/4\hbar$, if the photon energy E is much larger than both temperature and Fermi energy ε_F. Both conditions are stringently satisfied in our visible-optics experiments. The universal value of G also implies that all optical properties of graphene (its transmittance T, absorption P and reflection R) can be expressed through fundamental constants only (T, P and R are unequivocally related to G in the 2D case). In particular, it was noted by Kuzmenko *et al* (*S9*) that $T = (1+2\pi G_0/c)^{-2} = (1+0.5\pi\alpha)^{-2} \approx 1-\pi\alpha$ for the normal light incidence. We emphasize that – unlike G – both T and R are observable quantities that can be measured directly by using graphene membranes.

To find accurate absolute values of T and G, in the analysis shown in Figs. 1B and S2, we have omitted the part of the transmittance spectra at λ <450 nm, which as discussed above was affected by hydrocarbon contamination. Also, our apparatus noise was somewhat higher in the infrared region so that, after including the infrared data, the statistical error usually grew rather than decreased. Accordingly, we restricted the analysis to λ <800nm to maximize the accuracy. As a result, we have found $T \approx 97.7\%$ with an accuracy of ±0.1% (see Fig. 1B). The related analysis for G yields $G \approx 1.01G_0$ over the white-light region (450 nm <λ <800 nm) and the statistical standard error of ±4% (Fig. S2).

The approximation of 2D Dirac fermions is valid only close to the Dirac point and, for higher energies ε, one has to take into account such effects in graphene's band structure as triangular warping and nonlinearity (*S11*). The triangular warping is significant even for E <<1 eV, and there is little left of the linear Dirac spectrum at ε approaching 5 eV. Therefore, for visible energies of 2 to 3 eV, which are already comparable with the nearest-neighbor hopping energy $t \approx 3$eV, one may expect the breakdown of the Dirac-fermion approximation used in the calculations of G_0. Accordingly, the only earlier theory analysis that did take into account the finite-E corrections was limited to the infrared region (*S9*). For the purpose of our experiments, we have extended the theory to visible frequencies and, also, took into account the next-near-neighbor hopping (the latter was found to result only in minute corrections) (see ref. (*S10*) for details). Figure S4 shows the calculated dynamic conductivity G and light transmittance T with the finite-E effects included. One can see a noticeable increase in G at finite E with respect to its idealized value of $e^2/4\hbar$ but the corrections still do not exceed 2% for green light. Note that, in the infrared region, the corrections do not disappear but decrease relatively slowly (as $\propto E^2$), until one needs to take into account finite temperature and ε_F (*S6-S10*). Our calculations are also in quantitative agreement with the earlier analysis for E <1 eV (*S9*).

Now we turn our attention to few-layer graphene. It is surprising that its opacity is proportional to the number N of layers involved, at least, to a good approximation for $N \leq 4$ (see the inset in Fig. 1B). Indeed, electronic structures of the multilayer materials are different for different N. Generally, several energy bands are present for $N \geq 2$, and the interband distance is given by the energy of inter-plane hopping, $t_\perp \approx 0.3$ eV. This leads to complicated optical spectra with marked absorption peaks corresponding to interband transitions (*S9*, *S12*). However, for visible photon energies $E >> t_\perp$ the spectra significantly simplify so that up to corrections of the order of $(t_\perp/E)^2$ <<1 multilayer graphene can be considered as a stack of independent graphene planes. This leads to the opacity $(1 - T) \approx N\pi\alpha$. This expression was explicitly derived for bilayer graphene N =2 (*S10*) and, also, is apparent from Fig. 1 of ref. (*S12*). Further theoretical analysis is required for few-layer graphene.

Absorption of light by 2D Dirac fermions

Finally, we show how the universal value of graphene's opacity can be understood qualitatively, without calculating its dynamic conductivity first. Let a light wave with electric field $\vec{\Theta}$ and frequency ω fall

perpendicular to a graphene sheet of a unit area. The incident energy flux W_i is given by $W_i = \frac{c}{4\pi}|\Theta|^2$. Taking into account the momentum conservation $\boldsymbol{k}$ for the initial $|i\rangle$ and final $|f\rangle$ states, only the excitation processes pictured in Figure S5 contribute to the light absorption. The absorbed energy $W_a = \eta\hbar\omega$ is given by the number η of such absorption events per unit time and can be calculated by using Fermi's golden rule as $\eta = (2\pi/\hbar)|M|^2 D$ where M is the matrix element for the interaction between light and Dirac fermions, and D is the density of states at $\varepsilon = E/2 = \hbar\omega/2$ (see Fig. S5). For 2D Dirac fermions, $D(\hbar\omega/2) = \hbar\omega/\pi\hbar^2 v_F^2$ and is a linear function of ε.

The interaction between light and Dirac fermions is generally described by the Hamiltonian

$$\hat{H} = v_F \vec{\sigma}\cdot\vec{p} = v_F \vec{\sigma}\cdot(\hat{p} - \frac{e}{c}\vec{A}) = \hat{H}_0 + \hat{H}_{int}$$

where the first term is the standard Hamiltonian for 2D Dirac quasiparticles in graphene (*S11*) and $\hat{H}_{int} = -v_F \vec{\sigma}\cdot\frac{e}{c}\vec{A} = v_F \vec{\sigma}\cdot\frac{e}{i\omega}\vec{\Theta}$ describes their interaction with electromagnetic field. Here $\vec{A} = \frac{ic}{\omega}\vec{\Theta}$ is the vector potential and $\vec{\sigma}$ the standard Pauli matrices. Averaging over all initial and final states and taking into account the valley degeneracy, our calculations yield

$$|M|^2 = |\langle f| v_F \vec{\sigma}\cdot\frac{e}{i\omega}\vec{\Theta}|i\rangle|^2 = \frac{1}{8} e^2 v_F^2 \frac{|\Theta|^2}{\omega^2}.$$

This results in $W_a = (e^2/4\hbar)|\Theta|^2$ and, consequently, absorption $P = W_a/W_i = \pi e^2/\hbar c = \pi\alpha$, both of which are independent of the material parameter v_F that cancels out in the calculations of W_a. Also note that the dynamic conductivity $G \equiv W_a/|\Theta|^2$ is equal to $e^2/4\hbar$. Because graphene practically does not reflect light ($R \ll 1$ as discussed above), its opacity $(1 - T)$ is dominated by the derived expression for P.

In the case of a zero-gap semiconductor with a parabolic spectrum (e.g., bilayer graphene at low ε), the same analysis based on Fermi's golden rule yields $P = 2\pi\alpha$. This shows that the fact that the optical properties of graphene are defined by the fundamental constants is related to its 2D nature and zero energy gap and does not directly involve the chiral properties of Dirac fermions.

On a more general note, graphene's Hamiltonian $\hat{H}$ has the same structure as for relativistic electrons (except for coefficient v_F instead of the speed of light c). The interaction of light with relativistic particles is described by a coupling constant, a.k.a. the fine structure constant. The Fermi velocity is only a prefactor for both Hamiltonians $\hat{H}_0$ and $\hat{H}_{int}$ and, accordingly, one can expect that the coefficient may not change the strength of the interaction, as indeed our calculations show.

SUPPLEMENTARY FIGURES

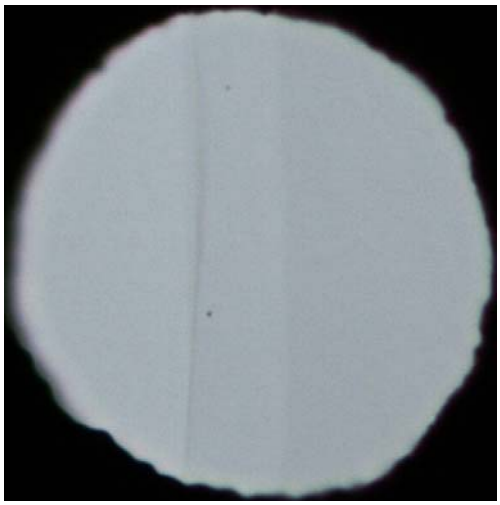

Figure S1. 50 μm aperture partially covered by graphene and its bilayer. This is the original photograph from Fig. 1A, as seen directly in transmitted white light in an optical microscope. No contrast enhancement or image manipulation has been used.

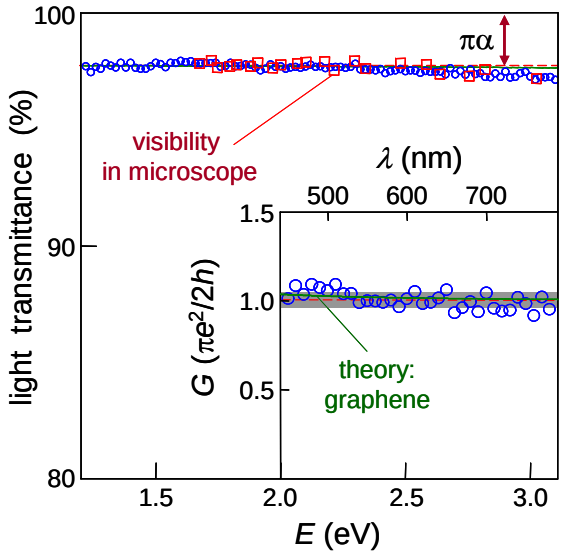

Figure S2. Transmittance spectrum of graphene over a range of photon energies E from near-infrared to violet. The blue open circles show the data obtained using the standard spectroscopy for a uniform membrane that completely covered a 30 μm aperture. For comparison, we show the spectrum measured using an optical microscope (red squares). The red line indicates the opacity of $\pi\alpha$. Inset: Dynamic conductivity G of graphene for visible wavelengths (symbols) recalculated from the measured T. The green curves in both main figure and inset show the expected theoretical dependences, in which G varies between 1.01 and 1.04 of $G_0 \equiv e^2/4\hbar$ for this frequency range. The red line and the gray area indicate the statistical average for our measurements and their standard error, respectively: $G/G_0 = 1.01 \pm 0.04$.

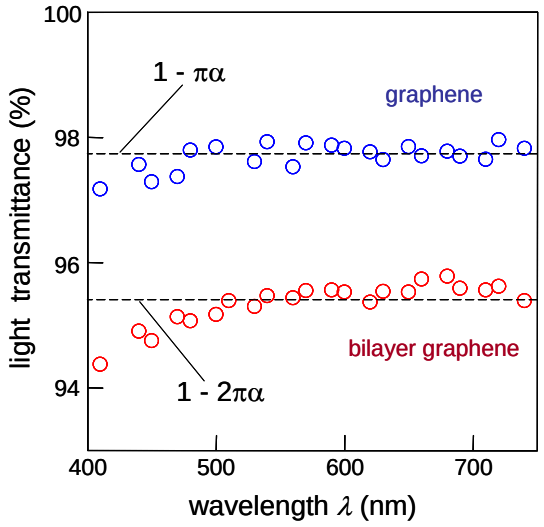

Figure S3. Transmittance spectra of single and bilayer regions of the sample shown in Fig. S1. The transmittance was measured by analyzing images taken in an optical microscope when the membrane was back-illuminated through narrow-band filters.

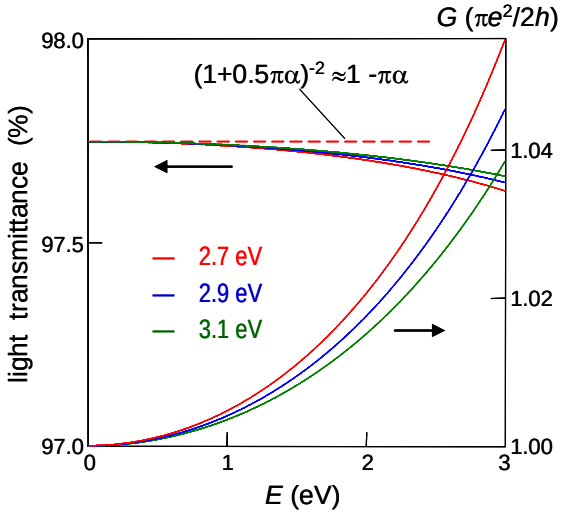

Figure S4. Dynamic conductivity as a function of photon energy E for graphene, taking into account its triangular warping and nonlinearity at finite energies ε. The curves are given for 3 values of t which cover the possible range expected for this hopping parameter. The corresponding curves for light transmittance are also shown. The red dashed line indicates the value for the idealized case of 2D Dirac fermions.

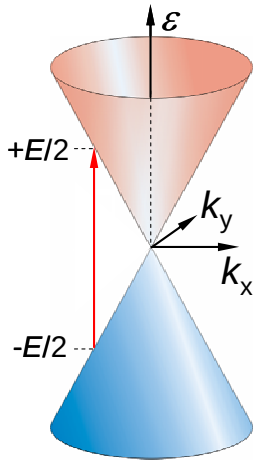

Figure S5. Excitation processes responsible for absorption of light in graphene. Electrons from the valence band (blue) are excited into empty states in the conduction band (red) with conserving their momentum and gaining the energy $E = \hbar\omega$.

SUPPLEMENTARY REFERENCES

S1. K. S. Novoselov *et al*, *Proc. Natl. Acad. Sci. USA* **102**, 10451 (2005).

S2. P. Blake *et al*, *Appl. Phys. Lett.* **91**, 063124 (2007).

S3. J. C. Meyer *et al*, *Nature* **446**, 60 (2007).

S4. J. S. Bunch *et al*, *Science* **315**, 490 (2007).

S5. M. Ishigami *et al*, *Nano Lett.* **7**, 1643 (2007).

S6. T. Ando *et al*, *J. Phys. Soc. Jpn* **71**, 1318 (2002).

S7. V. P. Gusynin *et al*, *Phys. Rev. Lett.* **96**, 256802 (2006).

S8. L. A. Falkovsky, S. S. Pershoguba. *Phys. Rev. B* **76**, 153410 (2007).

S9. A. B. Kuzmenko *et al*, *Phys. Rev. Lett.* (2008) (see arXiv:0712.0835).

S10. T. Stauber *et al*, arXiv:0803.1802.

S11. A. H. Castro Neto *et al*, *Rev. Mod. Phys.* (2008) (see arXiv:0709.1163).

S12. D. S. L. Abergel, V. I. Fal'ko. *Phys. Rev. B* **75**,155430 (2007).